Indian Journal of Biochemistry & Biophysics
Vol. 63, April 2026, pp. 442-452
DOI: 10.56042/ijbb.v63i4.22423

Synthesis of novel nanosized pharmacologically active macrocyclic complexes as efficient biomaterial

Vikas Sangwan*

Department of Chemistry, RPS Degree College-Balana, Mahendergarh-123 029, Haryana, India

Received 06 August 2025; *revised 09 November 2025*

Antimicrobial resistance is becoming prominent issues nowadays. Because of the requirement of new antimicrobial compounds a series of novel macrocyclic complexes of Ni^{II} and Cu^{II} with sulphur and nitrogen containing ligand have been prepared by divalent transition metal ion-mediated template method. The macrocyclic ligand is derived from the 4,6-Dihydroxy-2-mercaptopyrimidine (DMP) and thiosemicarbazide (TSC). Various physico-analytical and spectroscopic techniques like Infra-red spectroscopy, Electron Spray Ionisation-MS, Elemental analysis, UV-visible, EPR, Magnetic moment measurements and Molar conductivities were used for the structural depiction of the newly synthesized metal complexes. The assistance of PX-Ray-D technique was taken for the morphological study of Ni^{II} complex. Minimization of energy and numerous parameters for quantum chemical were calculated using the Gaussian 09 program. Based on several characterization,distorted octahedral geometries have been projected for all the metal complexes with assigned molecular formula [M ($C_{10}H_{14}N_{10}S_4$) X_2] where X= Cl^-, NO_3^- and CH_3COO^-. All the newly prepared metal complexes were screened for their bio-efficacy against some pathogenic strains of bacteria and fungus. *In silico* molecular docking studies were also performed against SARS- Cov-2 protein.

Keywords: Antimicrobial efficacies, Divalent metal ions, Template methodology

Transition metal ion prompted macrocyclic complexes have attracted extensive interest in the well-known area of coordination chemistry[1,2]. These complexes possess a widespread range of applications in the field of biological, industrial and pharmacology[3]. In the formation of macrocyclic complexes a key or prominent role have been shown by numerous factors like nature of the donor atom, the size of the cavity, and rigidity of the macrocycle[4,5]. A large no. of application of macrocyclic complexes in the area of radio therapeutic, catalysis and medical imaging have been reported[6]. Very well-known antimicrobial applications are imparted by these complexes[7-8]. There is the significant stability of the macrocyclic complexes having nitrogen atom[9]. The present literature states that Zn (II) complexes have good antibacterial activities[10]. The field of research that deals with the macrocyclic complexes are very wide and broad because of impending curiosity in many areas that involves bio-inorganic chemistry. Over the past decades, several antimicrobial drugs have been synthesized. Macrocyclic metal complexes are of tremendous interest for their contributions to material sciences because of their potential applications in both basic and practical sciences[11]. Their structural adaptability makes it possible to precisely alter characteristics like solubility, stability, and reactivity, which makes them indispensable for the development of novel molecules in the pharmaceutical and industrial industries[12]. These macrocyclic complexes have been proven potential to reduce the toxicity caused by pesticides[13]. After this, there are still various issues that are not being addressed by current antimicrobials. The designing and synthesizing of advance potential and potent antimicrobial medications is the need of a presentgeneration[14,15]. Prompted from the above uses and applications we have designed and synthesized a library of macrocyclic complexes and examined them for diverse biological activities.

*Correspondence:
E-mail: vikassangwan616@gmail.com
Suppl. data available on respective page of NOPR
Abbrevations: DMP, 4,6-Dihydroxy-2-mercapto pyrimidine; EPR, Electron Paramagnetic Resonance; ESI-MS, Electron Spray Ionisation Mass Spectrometry; HOMO, Highest Occupied Molecular Orbital; LUMO, Lowest Unoccupied Molecular Orbital; MTCC, Microbial Type Cultue Collection; PXRD, Powder X Ray Diffraction; SARS- Cov-2, Severe Acute Respiratory Syndrome Covid; TGA, Thermogravimetric Analysis; TSC, thiosemicarbazide; UV, Ultraviolet

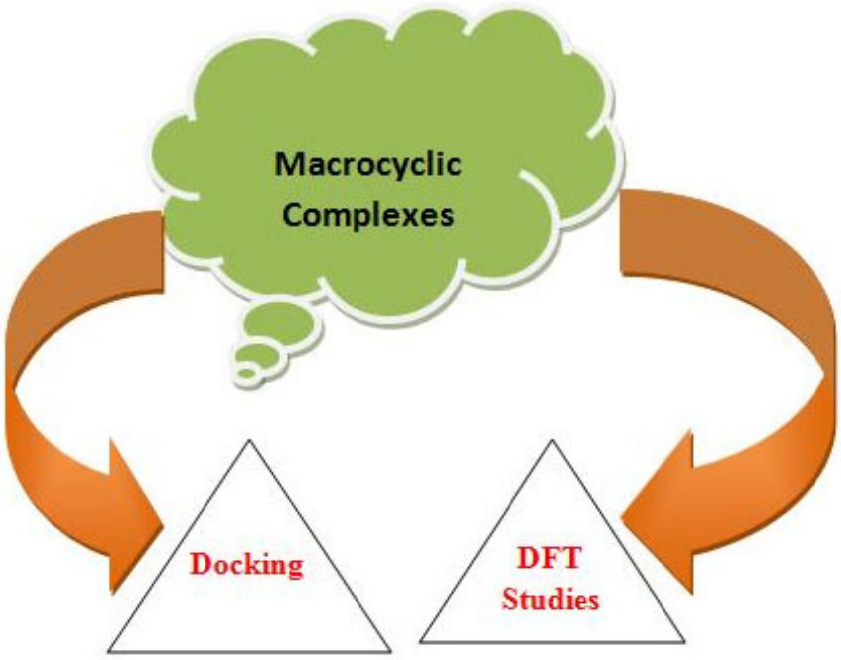

Graphical abstract

Experimental protocol

Materials and Method

The salts of divalent metals used in the present synthesis were procured from E. Merck, Ranbaxy, India and S. D. fine Mumbai, India. 4,6-Dihydroxy-2-mercaptopyrimidine (DMP) and Thiosemicarbazide (TSC) were purchased from Sigma Aldrich. Organic solvents like methanol, diethyl ether, dimethylformamide (DMF) and DMSO were of reagent grade and used as such received with no additional purification.

The IR spectrum was captured using KBr pellets on an FTIR spectrophotometer (Shimadzu) in the 4000-400 cm^{-1} range. The electrical melting point equipment was used to determine M.P. (melting points) with the use of capillaries. Carbon, Hydrogen, and Nitrogen microanalyses (CHN) were performed on a Euro EA elemental analyzer and metal content is determined by well-known literature method. Molar conductance values were forecasted using a digital conductivity metre (HPG System, G-3001). The study of the metal content of the complexes was done using literary techniques. At STIC-Cochin, measurements of magnetic susceptibility were taken. Electronic spectra (DMSO) were captured using a Thermo Scientific Evolution 201 Spectrophotometer. The complexes mass spectra were captured using the XEVO G2-XS QTOF device. PXRD data were collected using the Pan-Analytical XPERT-PRO instrument at. The Gaussian 09 programme was used for computational research, and quantum chemical parameters were determined.

Synthesis of the macrocyclic complexes

By using the divalent transition metal ion as a template for the product's cyclization, all the metal complexes were prepared (template methodology) [16-18]. Thiosemicarbazide, 1.05 g (10 mmol), was dissolved in 25 mL of methanol, and to this solution, metal salt, 5 mmol solution in methanol, was added drop by drop. The reaction mixture was then allowed to reflux for 35 to 45 min over a water bath. Strong color changes are a sign that the diamine moiety and the metal ion are coordinated. The aforesaid mixture was then given a dose of 1.44 g (10 mmol), and it was left to reflux for another 6 to 8 hrs. The response was now given the night to cool in desiccators. As a result of further washing, the varied colored powders were obtained. The reaction was now given a chance to cool over-night in desiccators. The diverse colored powder was produced, and unreacted reactants were eliminated through additional washing with various solvents. All metal complexes were synthesized using a similar methodology. The probable reaction's mechanism is depicted in (Fig. 1).

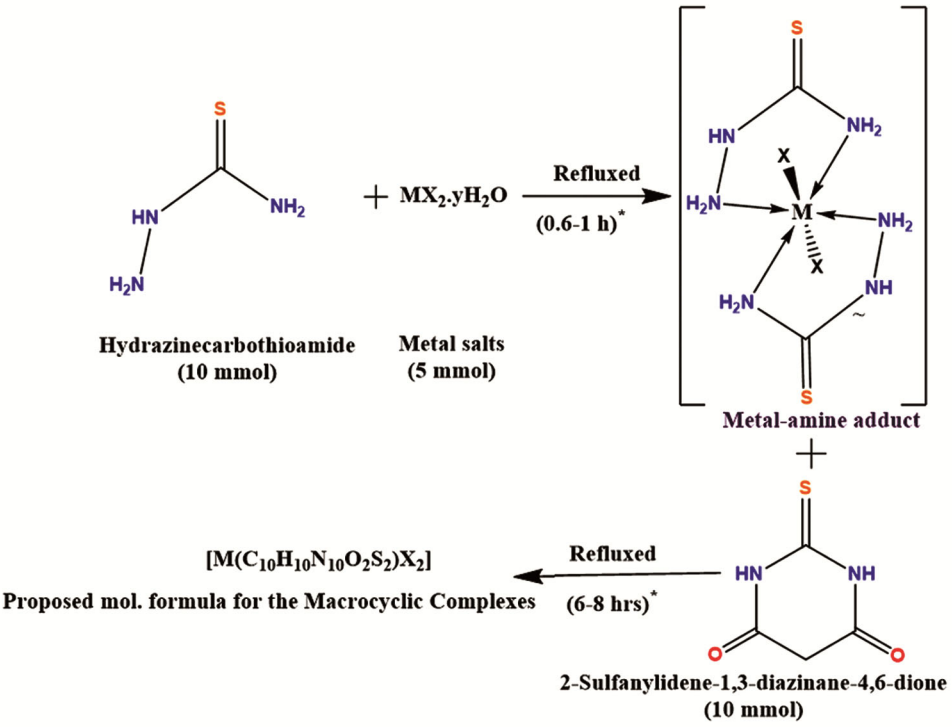

Fig. 1 — The general mechanism of the reaction

Biological studies

Test microorganisms

The bactericidal and fungicidal efficacy of each of the freshly made metal complexes against six harmful microbial strains was evaluated. The strains were chosen based on their pharmacological potential to cause various human illnesses. *Bacillus subtilis* (MTCC 121) and *Staphylococcus aureus* (MTCC 96) are the two gram-positive bacterial strains used in this study. Two gram-negative bacterial strains were *Escherichia coli* (MTCC 1652) and *Pseudomonas aeruginosa* (MTCC 741). Two fungal strains were also used, which were *Candida albicans* (MTCC 3017) and *Saccharomyces cerevisiae* (MTCC 170) (yeast strains). All of the microbial strains were purchased from IMTECH, Chandigarh's Microbial Type Culture Collection (MTCC).

Primary Screening

The antibacterial properties of the generated macrocyclic complexes[19] were evaluated using agar well diffusion. The 0.5 McFarland standard, or approximately 1.5 × 108 CFU/mL of microbial solution, was reached by all of the microbe cultures. 20 mL of agar media was added to each Petri plate, seeded with 100 µL inoculate of the test microorganisms, and then allowed to adsorb for 15 min. A sterile cork borer with an 8mm diameter was used to drill holes in the seeded agar plates. One volume containing 2.0 mg/mL doses of each chemical reconstituted in DMSO was then added to the wells. Every plate was incubated at 37°C for a full day. The antibiotic activity of each complex was evaluated using a zone reader and the zone of growth inhibition against the test organisms (HI Antibiotic zone scale). Amphotericin-B and ciprofloxacin were used as positive controls for bacteria and yeast, respectively, while DMSO served as a negative control. This method was performed on three replicate plates[20] for every organism.

Determination of Minimum Inhibitory Concentration (MIC)

The minimum inhibitory concentration (MIC) is defined as the lowest concentration of a compound required to inhibit the visible growth of a microorganism after overnight incubation. Complexes that demonstrated positive activity during primary screening were selected for MIC determination. The MIC of the synthesized complexes against selected bacterial and yeast strains was evaluated using a modified agar well diffusion method, as previously described in the literature. Briefly, a twofold serial dilution of each synthesized compound was prepared by initially dissolving the compound in dimethyl

sulfoxide (DMSO), followed by dilution with sterile distilled water to obtain concentrations ranging from 100 to 6.25 µg/mL. Agar plates were seeded with 100 µL of standardized microbial inoculum (1×10^6 CFU/mL). Each concentration of the test compound was added in triplicate to the wells bored into the inoculated agar plates. The plates were then incubated aerobically at 37°C for 24 h, after which zones of inhibition were examined. The MIC was recorded as the lowest concentration of the compound that completely inhibited visible microbial growth, indicated by a clear and distinct zone of inhibition. Amphotericin B and Ciprofloxacin were used as positive controls, while DMSO served as the negative control.

Molecular docking studies

Molecular docking studies were performed to gain deeper insight into the interaction and binding affinity of the synthesized complexes with target proteins. Docking simulations were carried out using AutoDock Vina, which employs an efficient search algorithm combined with a scoring function to predict optimal ligand conformations within the binding site of a protein. A blind docking approach was adopted by defining a grid box that encompassed the entire protein surface. The crystal structure of NSP15 endoribonuclease from SARS-CoV-2 was retrieved from the RCSB Protein Data Bank (PDB ID: 6VWW; DOI: 10.2210/pdb6VWW/pdb) for use in docking calculations. The three-dimensional structures of the synthesized compounds were drawn and geometry-optimized using ChemDraw 16. Protein and ligand preparation was performed using AutoDock Tools 1.5.6. Polar hydrogen atoms were added, Kollman and Gasteiger partial charges were assigned where appropriate, and the structures were saved in pdbqt format for docking analysis. The docking results were analyzed based on binding energy values and interaction patterns. The three-dimensional binding interactions between the target protein and the synthesized complexes were visualized and analyzed using PyMOL[21].

Results

The solubility of all the macrocyclic complexes was found to be good in DMSO and insoluble in common organic solvents. The non-electrolytic behavior of the complexes was confirmed by the lower value of molar conductance generally in the range of 12-24 $\Omega^{-1}cm^2mol^{-1}$. The elemental analysis and mass spectra result pointing towards the monomeric nature of the complexes. points of all temperature are above 200°C.

Physico-analytical data

Complex (**M1**) [Ni ($C_{10}H_{14}N_{10}S_4$) Cl_2]

Yield: 67 %, Mol. Wt. 495.97; Anal. Found: C, 24.01; H, 1.99; N, 28.07; M, 11.70 % Calc.: C, 24.22; H, 2.03; N, 28.24; M, 11.83. Color, Greyish green; Molar conductivity (Ω^{-1} $mol^{-1}cm^2$) in DMSO 14. Magnetic moment μ_{eff} (BM) : 3.01.

Complex (**M2**) [Ni ($C_{10}H_{14}N_{10}S_4$) (NO_3^-)$_2$]

Yield: 59 %, Mol. Wt. 549.08; Anal. Found: C, 21.68; H, 1.79; N, 30.54; M, 10.42% Calc.: C, 21.87; H, 1.84; N, 30.61; M, 10.69. Color, Purple red; Molar conductivity (Ω^{-1} $mol^{-1}cm^2$) in DMSO 13. Magnetic moment μ_{eff} (BM) : 2.98.

Complex (**M3**) [Ni ($C_{10}H_{14}N_{10}S_4$) (OAc)$_2$]

Yield: 62 %, Mol. Wt. 543.16; Anal. Found: C, 30.72; H, 2.85; N, 25.42; M, 10.69% Calc.: C, 30.96; H, 2.97; N, 25.79; M, 10.81. Color, Brick red; Molar conductivity (Ω^{-1} $mol^{-1}cm^2$) in DMSO 18. Magnetic moment μ_{eff} (BM) : 3.04.

Complex (**M4**) [Cu ($C_{10}H_{14}N_{10}S_4$) Cl_2]

Yield: 67 %, Mol. Wt. 498.91; Anal. Found: C, 23.86; H, 1.98; N,27.83 ; M, 12.44% Calc.: C, 23.98; H, 2.01; N, 27.97; M, 12.69 Color, Light brown; Molar conductivity (Ω^{-1} $mol^{-1}cm^2$) in DMSO 12. Magnetic moment μ_{eff} (BM) : 1.96

Complex (**M5**) [Cu ($C_{10}H_{14}N_{10}S_4$) (NO_3^-)$_2$]

Yield: 70 %, Mol. Wt. 553.93; Anal. Found: C, 21.54; H, 1.80; N, 30.27; M, 11.31% Calc.: C, 21.68; H, 1.82; N, 30.34; M, 11.47. Color, Brown; Molar conductivity (Ω^{-1} $mol^{-1}cm^2$) in DMSO 19. Magnetic moment μ_{eff} (BM) : 2.02.

Complex (**M6**) [Cu ($C_{10}H_{14}N_{10}S_4$) (OAc)$_2$]

Yield: 74 %, Mol. Wt. 548.01; Anal. Found: C, 30.60; H, 2.90; N, 25.52; M, 11.46% Calc.: C, 30.68; H, 2.94; N, 25.56; M, 11.60. Color, Blackish brown Molar conductivity (Ω^{-1} $mol^{-1}cm^2$) in DMSO 24. Magnetic moment μ_{eff} (BM) : 1.98.

IR Spectrum

The IR spectrum of all the macrocyclic complexes showed the absence of peak near 3400 cm^- due to free amine[22] and appearance of the new band at nearly 1600-1610 indicates about the condensation reaction and peak can be ascribed to the azomethine peak. (Fig. 2 and Suppl. Fig. S1). The lower drift in frequency

of the azomethine peak is because of the coordination of nitrogen atom with the metal ion. The peak near 1640-1650 and 3200-3260 cm^{-}may be attributed to the amide –I ν C=O and secondary amide N-H group present in the macrocyclic moiety. Amide –II [ν (C-N)] +δ (N-H) and amide III (N-H) band occurred at 1400, 1346 and 704 cm^{-1}. Presence of peak for the free C=O ruling out the possibility of condensation of both the carbonyl group of the amine acid[23,24].

ESI-MS

The mass spectrum of the[Ni ($C_{10}H_{14}N_{10}S_4$) OAc_2] and [Cu ($C_{10}H_{14}N_{10}S_4$) Cl_2] was recorded and studied as a representative case. (Fig. 3 and Suppl. Fig. S2).

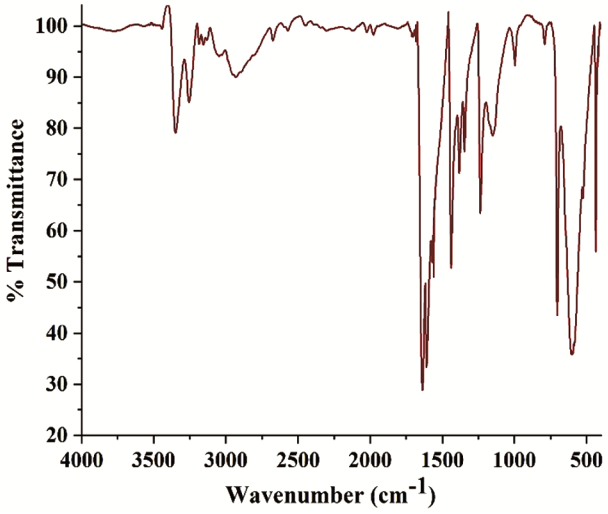

Fig. 2 — IR spectrum of the complex [Ni ($C_{10}H_{14}N_{10}S_4$) Cl_2]

The molecular ion peak of the complexes was observed at 544.85 and 496.80 corresponding to m/z expected at 543.09 and 498. The mass spectrum reveals the monomeric nature of the complex and also ruled out the possibility of the condensation of C=O group instead of C=S.

Electronic spectra

Nickel nitrate

At room temperature, the value of magnetic moment for the Nickel (II) complexes lies in the range of 2.95-3.05 B.M. These values of magnetic moments showed the presence of two unpaired electrons that is further explained on the bases on absorptionin UV-Visible spectra. (Suppl. Fig. S3). In the absorption spectrum of the Ni (II) complexes in DMSO as a solvent, the bands appeared at nearly 1050, 950, 580,400 and 320 nm. That can be designated to the $^3A_{2g}$ (F) → $^3T_{2g}$ (F) (ν1), $^3A_{2g}$ (F) → $^3T_{1g}$ (F) (ν2), and $^3A_{2g}$ (F) → $^3T_{1g}$ (P) (ν3) and higher energy band can be ascribed to charge transfer and π→π* transition, respectively[25]. The results demonstrate about the octahedral environment around the metal ion.

Copper nitrate

In case of Cu (II) complex band are presented at 730-800 and 325 nm that may be due to d-d transition ($^2B_{1g}$ → $^2A_{1g}$) and π→π* respectively. (Suppl. Fig. S4). The magnetic moment values lie in between 1.95-2.02 B.M. that reveals about the presence of one unpaired electron and an octahedral geometry around the metal ion[26].

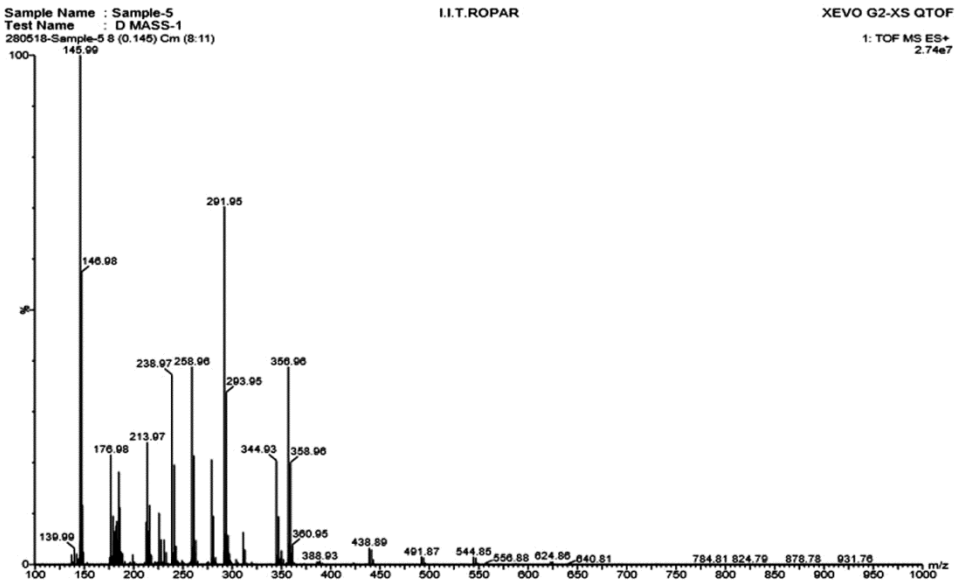

Fig. 3 — Mass spectrum of the complex [Ni ($C_{10}H_{14}N_{10}S_4$) $(OAc)_2$]

PXRD analysis

Even after several attempts, the development of a single crystal of the synthesized macrocyclic complexes has not been achieved; therefore, a powder XRD examination was conducted in the range of 5-90° (2) in order to determine the nature of the complexes (crystalline or amorphous). Figure 4 displays the representative Ni (II) complex's powder X-ray diffractogram at room temperature. The full proof suite software was used for the evaluation or calculation of the various cell parameters like h,k,l, and d-spacing. The given complex is possessing the triclinic crystal system with the lattice parameters as a= 9.1119, b= 8.3959, c = 7.2537 and α =112.743 β = 85.787, γ = 107.389. The presence of large numbers of peaks in the diffractogram is pointing towards the good crystalline nature of the complex.

The grain size of the complexes

Debye-Scherrer formula[27-29] was used to calculate the size of a particle of the synthesized macrocyclic complexes, and it may be mathematically expressed as:

$D = 0.94 \lambda / \beta \cos\theta$

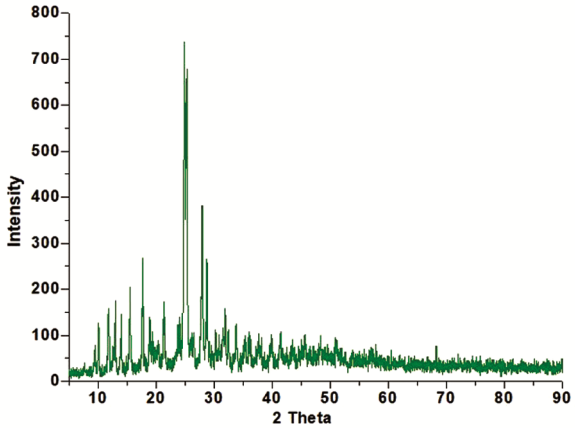

Fig 4 — PXR diffractogram of the complex [Ni ($C_{10}H_{14}N_{10}S_4$) $(OAc)_2$]

In the above-mentioned equation

β = is the full width at half maximum (FWHM) of the given XRD peak (characteristic)

λ = is the incident X-ray wavelength

D = is the apparent particle size cosθ = position of the particular diffraction peak

Based on the information provided, we determined that the value of λ is 1.54 (A°) and the value of β is in (radians). The diffractogram shows the value of cos θ. According to our estimates, the particle size spans from 34 nm to 0.0049, while the lattice strain has a value in the same range (Table 1).

EPR spectrum

The EPR spectrum of the Cu (II) complex was taken on X-band frequency of 9.1 GHz at room temperature. The spectrum showed an anisotropic signal with the $g_{\parallel}$ = 2.1013and g⊥ = 2.0483. The observed values of g reveal that the unpaired electron resides in d_x^2-y^2 and the metal ion is having d^9 configuration. (Suppl. Fig. S5). The condition of tetragonal distortion holds good because g (tensor) follows the order of $g_{\parallel} > g \perp > 2.0023$. The $g_{average}$ and G values for the complex are 1.3832 and 2.144 showing covalent environment and Cu-Cu interaction in the polycrystalline phase[30,31].

TGA

Thermogravimetric analysis was used to determine the thermal stabilities of the macrocyclic complexes in the temperature range of 50-800°C while maintaining a heating rate of 10°C/min. Pt pans were utilized, and the N_2 environment was preserved. The metal complexes were broken down in two phases.

The lack of weight loss between 50 and 200°C points to the absence of water molecules in both typical complexes. In case of complex M2 (Fig. 5) first degradation step occurred in between 210-250°C and

Table 1 — Interplanar spacing and Miller indices

H	K	L	DOBS	DCAL	DOBS-DCAL	2TH.OBS	2TH.CAL	DIF.2TH
1	0	0	8.73218	8.74214	-0.0099	10.122	10.110	0.012
0	1	0	7.45167	7.44173	0.00993	11.867	11.883	-0.016
0	0	1	6.72386	6.71539	0.00846	13.157	13.173	-0.0017
1	-1	0	-	6.72024	0.00362	-	13.164	-0.007
0	1	-1	6.32458	6.33422	-0.0096	13.991	13.970	0.021
1	-1	1	5.70898	5.71169	-0.0027	15.509	15.501	0.007
1	1	0	4.98310	4.97734	0.00577	17.785	17.806	-0.021
1	-1	-1	4.14363	4.14323	0.00041	21.427	21.429	-0.002
1	1	1	3.53875	3.54020	-0.0014	25.145	25.135	0.010
1	-2	2	3.18939	3.18737	0.00202	27.952	27.970	-0.018
1	2	0	3.09879	3.09913	-0.0003	28.787	28.784	0.003
1	-3	1	2.80332	2.80417	-0.0008	31.898	31.888	0.010

62.04% wt. loss was observed that may be due to the loss of organic moiety $C_8H_5N_7O_5S_2$ and in the second step over the temp. the range of 260- 585°C having wt. loss of 7.59% may be due to $C_2H_3N_1$moiety. In the case of M4 (Suppl. Fig. S6) complex first degradation occurred at 200-290°C having a wt. loss of 48.88% because of $C_5H_5N_8S_2$ moiety and in 25 % wt. loss in temperature between 360-690°C corresponds to $C_5H_5N_2Cl$ organic framework.

Computational studies

Geometry optimization of the structures

The structures of the two representative macrocyclic complexes were optimized (Fig. 6) by using B3LYP at LAND2Z basis set. The minimized energy for the Ni (II) and Cu (II) complexes are -1304.24 and -1331.08 a.u. The selected bond length and bond angle parameters were calculated and presented in (Tables 2 & 3).

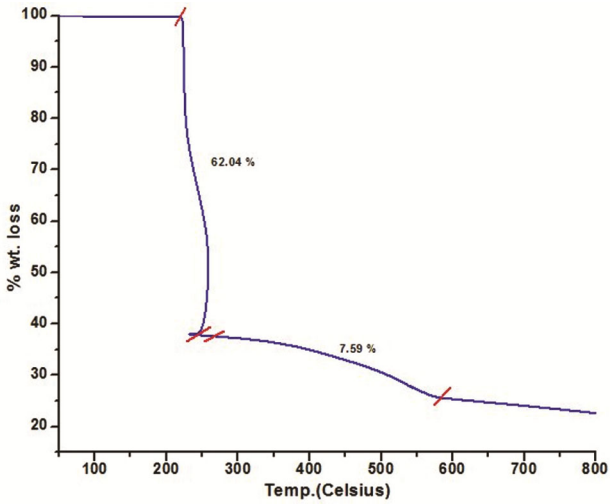

Fig. 5 — TGA graph of the complex [Ni ($C_{10}H_{14}N_{10}S_4$) (NO_3^-)$_2$]

Frontiers Molecular Orbitals (HOMO-LUMO)

The HOMO and LUMO play an intriguing role in the material's electrical and optical properties. (Fig. 7) Despite this, it is important, just as it is in quantum chemistry[32]. A crucial stability indicator, the energy gap ΔE (HOMO-LUMO) is widely useful for creating theoretical models to clarify the conformational and structural barriers in many molecular systems. On the basis of ΔE, the compound's reactivity can be quickly assessed. The quantum chemical parameter is depicted (calculated Table 4). The following equation was used to determine a number of additional parameters, including electronic charge (N_{max}), absolute hardness (η), global softness (S), absolute electronegativity (χ), global electrophilicity (ω) and separation energy (E) (i-viii)

$\Delta E = E_{LUMO} - E_{HOMO}$ (i)

$\chi = -(E_{HOMO} + E_{LUMO})/2$ (ii)

$\eta = (E_{LUMO} - E_{HOMO})/2$ (iii)

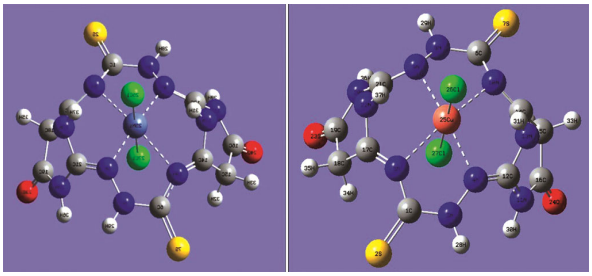

Fig. 6 — Optimized geometry of complex [Ni ($C_{10}H_{14}N_{10}S_4$) Cl_2] (LHS) and [Cu ($C_{10}H_{14}N_{10}S_4$) Cl_2] (RHS)

Table 2 — Bond angles parameters of the representative complex

S. No	Bond angles Ni (II) Complex		Bond angles Cu (II) Complex	
1	5 N – 25 Ni – 25 Cl	98.21	26 Cl – 25 Cu – 27 Cl	179.58
2	9N-25 Ni – 27 Cl	84.52	26 Cl – 25 Cu – 5 N	101.13
3	9 N- 25 Ni -10 N	73.34	20 N – 19 C – 23 O	119.92
4	5 N – 1 C- 2 S	126.80	5 N – 1 C – 2 S	125.83
5	11 N- 16 C -15 C	117.86	16 C – 15 C – 14 C	112.27
6	20 N – 21 C – 9 N	129.96	10 N – 25 Cu – 9N	72.63

Table 3 — Bond length parameters of the representative complex

S. No	Bond lengths Ni (II) Complex		Bond lengths Cu (II) Complex	
1	25 Ni – 5 N	2.47	25 Cu – 26 Cl	2.30
2	25 Ni – 9 N	1.98	25 Cu – 5N	2.32
3	25 Ni – 26 Cl	2.25	9 N – 21 C	1.31
4	5 C – 7 S	1.71	6 C – 7 S	1.71
5	1 C – 2 S	1.71	19 C – 23 O	1.23
6	19 C – 23 O	1.23	3 N – 1 C	1.38
7	15 C – 24 C	1.23	25 Cu – 4 N	2.18

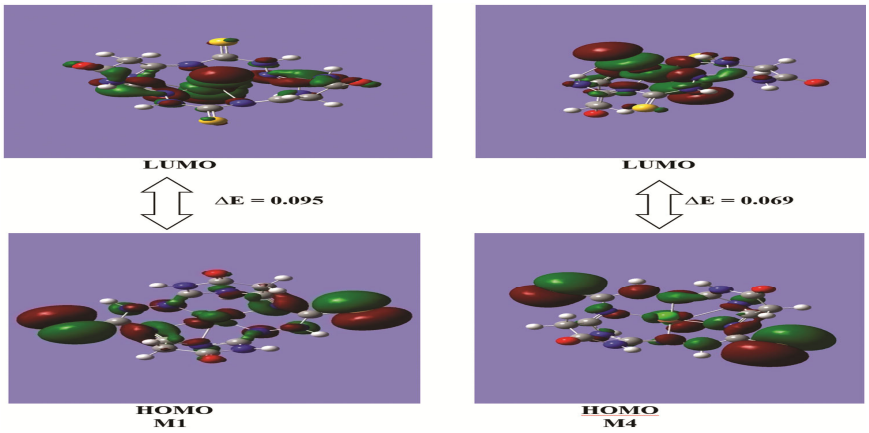

Fig. 7 — HOMO-LUMO of the complexes

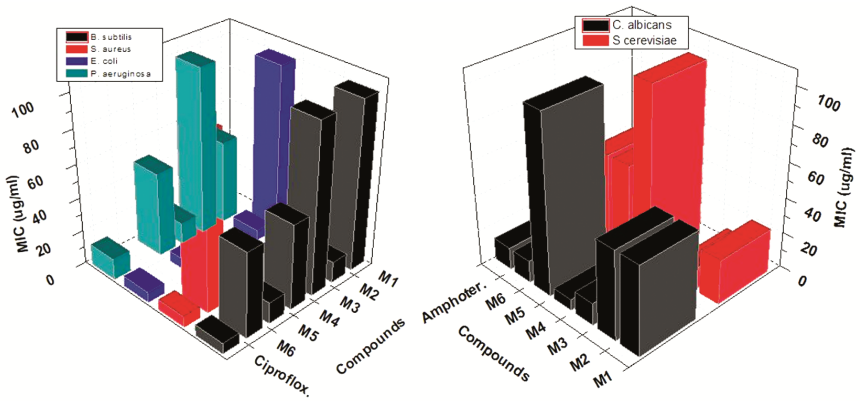

Fig. 8 — Pictorial representation showing MIC of the newly prepared complexes

Table 4 — Quantum chemical parameters

Complex	HOMO	LUMO	ΔE	χ	η	σ	*Pi*	S	ω	ΔN_{max}
M1	-0.242	-0.147	0.095	0.195	0.047	20.96	-0.195	10.48	0.398	4.090
M4	-0.250	-0.181	0.069	0.215	0.034	28.86	-0.215	14.43	0.671	6.223

$\sigma = 1/\eta$ (iv)

$Pi = -\chi$ (v)

$S=1/2\ \eta$ (vi)

$(\omega) = Pi^2/2\ \eta$ (vii)

$\Delta N_{max} = -Pi/\eta$ (viii)

Biological assay

Antimicrobial studies

All the newly prepared macrocyclic complexes are screened for *in vitro* antimicrobial activities against the pathogenic strains of bacteria and fungi. All the complexes showed fair activity against all the microbes used in the present study. Compound M1 and M5 exhibited overall good activity. The activity is compared with the well-known drugs available in the market like Ciprofloxin and Amphotericin. (Fig. 8 and Suppl. Table S1). The action of the complexes can be easily explained by the Tweedy's Chelation Theory that states that the increase in nonpolar character in compounds better is its efficiency to penetrate the cell membrane of the microbes. So after chelating, the electropositive character of the metal ion is decreased and hence showed good activity.

Table 5 — Binding energy of the complexes in enzyme pocket

Complex	Binding energy ((kcal/mol)
M1	-8.1
M2	-8.4
M3	-8.9
M4	-7.6
M5	-8.1
M6	-8.1

Molecular docking

Autodock Vina conducted research on protein interactions[33]. All complexes' binding energies are

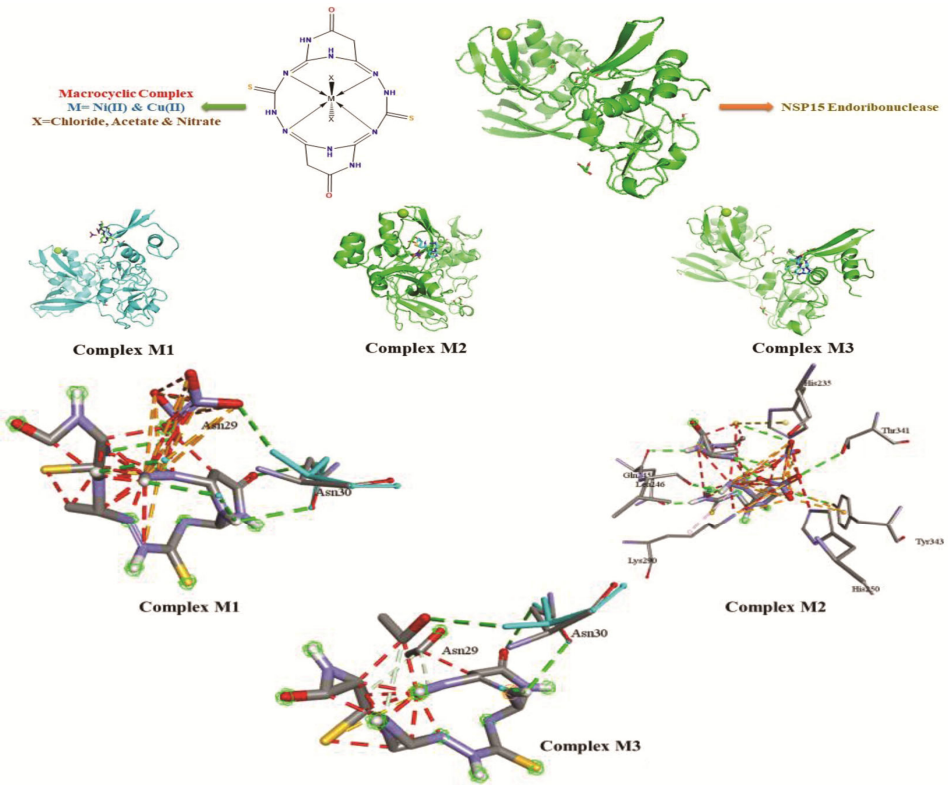

Fig. 9 — Docked structure of Complexes (M1-M3) with enzyme and site of interaction

listed in the table. Number Five Complex M3 fits the enzyme pocket the best and has the lowest binding energy of all the studied complexes (Table 5). Complex M3 uses the H-Bonding to bind with the amino acid asparagine[34,35]. Figure 9 Similarly, the other complex M1 interacts with the amino acid asparagine at the same location. The complex M2 interacts at various binding site like His 35, Thr 341, Leu 246, Tyr 343. In the similar way M4, M5 and M6 binds at different sites as shown in (Suppl. Fig S7).

Discussions

Elemental analysis and ESI-MS: Data revealed about the monomeric nature of the complexes. We got the values of elemental analysis in accordance with the expected calculated values.

Molar conductance: Data is in good agreement with the non-electrolytic nature of the complexes.

Infrared spectral studies: This study provide significant evidence regarding the coordination of synthesized macrocyclic ligand with the metal ion in a template method.

Electronic spectra & magnetic moment: This technique helps in evaluating the various type of electronic transitions possible in the synthesized complex. Magnetic moment values indicates the presence of unpaired electron in the complexes.

TGA: This is very beneficial technique to elucidate the thermal behavior of the complex along with various degradation steps involved. In the current study representative complex undergo two steps of degradation that corresponds to two organic moiety.

EPR: This spectroscopic technique imparts sufficient information regarding the distortion in the geometry and presence of unpaired electron in which orbital. The results obtained showed that complexes possess distorted octahedral geometry in case of Cu (II) complex.

PXRD: The particle size of the crystallite and crystalline behavior was elucidated by this technique. The given complex possess the triclinic crystal system with the lattice parameters as given above. The presence of large numbers of peaks in the diffractogram is pointing towards the good crystalline nature of the complex.

Computational studies: The assistance of this technique is taken in order to find out various energy parameters of the synthesized complex. HOMO-LUMO gap provides sufficient information regarding the reactivity of the complex.

Antimicrobial and docking studies: Molecular docking studies were performed to gain a better understanding of the binding efficacy of the synthesized complexes with target proteins. Antimicrobial activity was evaluated in terms of Minimum Inhibitory Concentration (MIC), which is defined as the lowest concentration of a compound required to inhibit the visible growth of a microorganism after overnight incubation. Complexes that showed positive results in the preliminary screening were further selected for MIC determination. All tested complexes demonstrated moderate antimicrobial activity against the selected microbial strains. Among them, compounds M1 and M5 exhibited comparatively better overall activity. Molecular docking analysis revealed that complex M3 possessed the lowest binding energy, indicating stronger binding affinity, and showed the best fit within the active site pocket of the target enzyme. Furthermore, complex M3 formed a hydrogen bond interaction with the asparagine amino acid residue, contributing to its stable binding within the enzyme active site

Conclusion

In the present study, we have synthesized and characterized macrocyclic complexes of Ni (II) and Cu (II). Geometry optimization and quantum chemical parameters were calculated by DFT studies. An octahedral geometry has been projected for all the complexes. Thermal behavior was determined by TGA studies. Biological screening of the complexes reveals good pharmacological activity. Good Docking activity was noticed al the complexes that points towards the applicability of the given complexes in SARS-Cov-2 treatment.

Conflicts of interest

The author declares no conflict of interest.

References

1 El-Boraey HA & EL-Gammal OA, Macrocyclic Cu (II) and Pd (II) complexes with new 16-membered tetradentate [N4] ligand: synthesis, characterization, 3D molecular modeling and *in vitro* anticancer and antimicrobial activities. *J Incl Phenom Macrocycl Chem*, 90 (2018) 123.

2 Kumar U & Chandra S,Synthesis, spectral and antifungal studies of some coordination compounds of cobalt (II) and copper (II) of a novel 18-membered octaaza [N8] tetradentate macrocyclic ligand. *J Saudi Chem Soc,* 15 (2011) 187.

3 Keypour H, Mahmoudabadi M, Shooshtari A, Bayat M, Mohsenzadeh F & Gable RW, Cadmium (II) macrocyclic Schiff-base complexes containing piperazine moiety: Synthesis, spectroscopic, X-ray structure, theoretical and antibacterial studies, *J Mol Struct,* 1155 (2018) 196.

4 Krishnapriya KR & Kandaswaswamy M, Coordination properties of a dicompartmental ligand with tetra- and hexadentate coordination sites towards copper (II) and nickel (II) ions. *Polyhedron*, 24 (2005) 113.

5 Lindoy LF, *The Chemistry of Macrocyclic Ligand Complexes,* Cambridge: Cambridge University Press, 1989.

6 Soni K, Singh RV & Fahmi N, Synthesis of new macrocyclic complexes of transition metals: Structural characterization and biological activity*, Russ J Gen Chem,* 87 (2017) 1610.

7 Singh RV & Chaudhary A, Biologically relevant tetraazamacrocyclic complexes of manganese: synthetic, spectral, antimicrobial, antifertility and antiinflammatory approach. *J Inorg Biochem,* 98 (2004) 1712.

8 Chaudhary A, Bansal N, Gajraj A & Singh RV, Antifertility, antibacterial, antifungal and percent disease incidence aspects of macrocyclic complexes of manganese (II). *J Inorg Biochem*, 96 (2003) 393.

9 Gull P, Babgi BA, Hashmi AA, Synthesis of Ni (II), Cu (II) and Co (II) complexes with new macrocyclic Schiff-base ligand containing dihydrazide moiety: Spectroscopic, structural, antimicrobial and antioxidant properties. *Micro Pathog,* 110 (2017) 444.

10 Keypour H, Mahmoudabadi M & Shooshtari A, Hosseinzadeh L, Mohsenzadeh F & Gable RW, Synthesis of Mn (II) and Zn (II) complexes with new macrocyclic Schiff-base ligands containing piperazine moiety: Spectroscopic, structural, cytotoxic and antibacterial properties. *Polyhedron* 127 (2017) 345.

11 Phor A, Gupta M & Chaudhary A, Design, synthesis, characterization, *in vitro* cytotoxic, antimicrobial, antioxidant studies, DFT, thermal and molecular docking evaluation of biocompatible Co (II) complexes of N4O4-macrocyclic ligands. *Comput Biol Chem,* 110 (2024) 108032.

12 Devi A, Mamta, Subhash, Gahlyan N, Aggarwal NK & Chaudhary A, Structure Synthesis, spectral characterization, density functional theory calculations, molecular docking studies and Biocidal evaluation of Schiff base Zn (II) and Cu (II) complexes. *J Mol Struc*, 1346 (2025) 143076.

13 Kumar J, Kumar R, Bhardwaj JK, Singh D, Kumar H & Jangra A, Kumar P, Development of Template-Assisted Biologically Active Macrocyclic Complexes: Structural Characterization and Apoptotic Studies. *Appl Organomet Chem*, 39 (2025) e70418.

14 Canali L & Sherrington DC, Utilisation of homogeneous and supported chiral metal (salen) complexes in asymmetric catalysis. *Chem Soc Rev,* 28 (1999) 85.

15 Gull P, Malik MA, Dar OA & Hashmi AA, Design, synthesis and spectroscopic characterization of metal (II) complexes derived from a tetradentate macrocyclic ligand: Study on antimicrobial and antioxidant capacity of complexes. *Microb Pathog*, 104 (2017) 212.

16 Yadav M, Yadav D, Singh DP & Kapoor JK, Macrocyclic Schiff Base Complexes of Zn (II), Cu (II), Co (II), and Ni (II) Targeting Topoisomerase IIβ: Synthesis, Docking, and Evaluation as Potential Anticancer Agents. *Appl Organomet Chem,* 39 (2024) e7885.

17 Yadav M, Yadav D, Singh DP & Kapoor JK, A salophen-type macrocyclic Schiff base ligand and its metal complexes:

exploring *in vitro* anticancer efficacy *via in silico* topoisomerase IIβ enzyme targeting. *Dalton Trans*, 54 (2025) 10358.
18 Yadav M, Yadav D, Kansal S, Angrup A, Taneja N, Singh DP & Kapoor JK, Pharmacologically important tetraaza macrocyclic Schiff base complexes of Zn (II), Cu (II) and Co (II) : Synthesis, characterization, DFT studies, molecular docking and *in vitro* anti-bacterial and anti-cancer studies. *J Mol Struct,* 1317 (2025) 139078.
19 Rahman AU, Chaudhary MI & Thomsen WJ, *Bioassay Techniques for Drug Development.* The Netherlands: Harwood academic Publishers, 2001.
20 AnejaKR, Sharma C & Joshi R, *In vitro* efficacy of amaltas (Cassia fistula L.) against the pathogens causing otitis extern.*Jund J Microbial*, 4 (2011) 175.
21 Pahonţu E, Proks M, Shova S, Lupaşcu G, Diana-Carolina I, Ştefania-Felicia B, Laura-Ileana S, Badea M, Păunescu V, Istrati V, Gulea A, Drăgănescu D & Pîrvu CED, Synthesis, characterization, molecular docking studies and *in vitro* screening of new metal complexes with Schiff base as antimicrobial and antiproliferative agents. *Appl Organometal Chem*33 (2019e5185.
22 Adam AMA, Alhadhrami1A, Saad HA & Refat MS, Synthesis and spectroscopic characterizations of Cu (II) complexes with novel 15-membered N4 macrocyclic ligand and their utility to obtain CuO nanostructures for efficient degradation of dyes. *Appl Organometal Chem,* 32 (2018) 3950.
23 Sangwan V & Singh DP, Trivalent transition metal ion mediated template synthesis: *In silico* molecular docking, DNA binding, antimicrobial evaluation and DFT studies. *Polyhedron*, 264 (2024) 117230.
24 El-Boraey HA, Coordination behavior of tetraaza [N4] ligand towards Co (II), Ni (II), Cu (II), Cu (I) and Pd (II) complexes: Synthesis, spectroscopic characterization and anticancer activity. *Spectrochim Acta A,* 97 **(**2012) 255.
25 El-Boraey HA & El-Din AAS,Transition metal complexes of a new 15-membered [N5] penta-azamacrocyclic ligand with their spectral and anticancer studies. *Spectrochim Acta A,* 132 (2014) 663.
26 Agarwal RK, Sharma D, Singh L & Agarwal H, Synthesis, Biological, Spectral, and Thermal Investigations of Cobalt (II) and Nickel (II) Complexes of N-Isonicotinamido-2′,4′-Dichlorobenzalaldimine *Bioinorg Chem App,* 3 (2006) 1.
27 Arjmand F & Aziz M, Synthesis and characterization of dinuclear macrocyclic cobalt (II), copper (II) and zinc (II) complexes derived from 2,2,2′,2′-S,S[bis (bis-N,N-2-thiobenzimidazolyloxalato-1,2-ethane)]: DNA binding and cleavage studies. *Eur J Med Chem*, 44 (2009) 834.
28 Lever ABP, *Inorganic electronic spectroscopy*, Amsterdam, London NY: Elsevier publishing company, 1986.
29 Ali MAEAA & Abu-Dief AM, CuFe2O4 nanoparticles: an efficient heterogeneous magnetically separable catalyst for synthesis of some novel propynyl-1H-imidazoles derivatives. *Tetrahedron,* 71 (2015) 2579.
30 Ahmed M, Abu-Dief, Ibrahim F & Elasyed WH, Magnetic NiFe2O4 nanoparticles: efficient, heterogeneous and reusable catalyst for synthesis of acetylferrocene chalcones and their anti-tumour activity. *Appl Organometal Chem,* 30 (2016) 917.
31 Abu-Dief AM, Mohammed SM, Abdelbaky MSM, Martínez-Blanco D, Amghouz Z & García-Granda B, Effect of chromium substitution on the structural and magnetic properties of nanocrystalline zinc ferrite. *Mater Chem Phys*, 174 (2016) 164.
32 Chandra S, Qanungob RK & Sharma SK, New hexadentate macrocyclic ligand and their copper (II) and nickel (II) complexes: Spectral, magnetic, electrochemical, thermal, molecular modeling and antimicrobial studies. *Spectrochim Acta A,* 94 (2012) 312.
33 Gurumoorthy P, Ravichandran J, Karthikeyan N, Palani P & Rahiman AK, Template Synthesis of Polyaza Macrocyclic Copper (II) and Nickel (II) Complexes: Spectral Characterization and Antimicrobial Studies. *Bull Korean Chem Soc*, 33 (2012) 2279.
34 Selmi W & Abdelhak J, Marchivie M & Zid MF, A comparative structural, spectroscopic, optical and photoluminescence studies by DFT of Fe (II) difluoro (oxalato) borate complex. *J Photochem Photobiol A*, 352 (2018) 43.
35 Trott O & Olson AJ, AutoDock Vina: improving the speed and accuracy of docking with a new scoring function, efficient optimization and multithreading. *J Comput Chem* 31 (2010) 455.